Kovove Mater. 50 2012 351–356
DOI: 10.4149/km_2012_5_351

Degradable Mg-Y-Nd-Mn alloys modified by Sc or Zn

I. Stulíková[1], B. Smola[1]*, F. Hnilica[2], V. Březina[3], L. Joska[4]

[1]*Faculty of Mathematics and Physics, Charles University, Ke Karlovu 3, 121 16 Prague 2, Czech Republic*
[2]*Faculty of Mechanical Engineering, Czech Technical University in Prague, Technická 4, 166 07 Prague 6, Czech Republic*
[3]*Institute of Physical Biology, University of South Bohemia, Zámek 136, 373 33 Nové Hrady, Czech Republic*
[4]*Faculty of Chemical Technology, Institute of Chemical Technology, Technická 5, 166 28 Prague 6, Czech Republic*

Received 8 December 2011, received in revised form 27 March 2012, accepted 28 March 2012

Abstract

Magnesium alloys have been recently recognized as a biodegradable material for bone substitute application. Degradation rates of Mg alloys in the physiological environment, mechanical properties and cytocompatibility are interesting research topics up to now as their combination limits most clinical applications. At least the first two properties are in a direct connection with structure and microstructure of proposed materials. Two variants of the commercial WE-type alloy (Mg-Y-Nd-Zr) modified by Mn addition and Zr absence and alloyed with either Sc or Zn were studied in the as cast as well as in the T5 condition in this work. Yield tensile stress and ultimate tensile stress values at room temperature for both alloys studied after the T5 temper are comparable with those in the T6 treated commercial WE43 alloy. Hardening is caused by precipitation of prismatic plates non-uniformly distributed in matrices of both alloys. Ductility of both alloys regardless the treatment increases essentially compared to the WE43 alloy. Thin coherent hexagonal plates containing Zn and Y in a high number density and with a very high aspect ratio developed parallel to matrix basal planes during the T5 temper in the as cast Mg-Y-Nd-Zn-Mn alloy. The extracts of the studied alloys in EMEM prepared according to the ISO 10993-5 are cytotoxic for human osteosarcoma MG63 cells. The worst result was obtained for the T5 treated Mg-Y-Nd-Zn-Mn alloy and can be ascribed to the enhanced corrosion connected with the observed microstructure. The viability of Mg63 cells improves considerably in the ten times diluted extract, which is more realistic for a comparison with *in vivo* testing due to dynamic effects.

K e y w o r d s: degradable Mg alloys, mechanical properties, corrosion, cytocompatibility

1. Introduction

Degradation in aqueous solutions and biocompatibility of magnesium render Mg alloys promising candidates for temporary implants [1, 2]. Material degradation and simultaneous implant replacement through the surrounding tissue in proper mutual rates are the essential conditions for such process. Recently research interests focus to high-strength Mg alloyed with non toxic elements and their corrosion products as to materials potentially used in osteosynthesis. Moreover, some physical properties as density or Young's modulus of Mg and its alloys are close to the human bone [3].

Two groups of Mg alloys selected on the ground of their technical applications are investigated *in vitro* and *in vivo* – Mg alloys with Al and Zn (AZ-type alloys, e.g. [4, 5]) and Mg alloys with rare earth (e.g. WE-type alloys [2, 5, 6], where the designation means Mg-Y-Nd). Some hesitations exist in implantations of aluminium containing magnesium alloys into humans due to a doubt that Al can induce the Alzheimer desease. Most rare earth elements, Mn and Zr, show a beneficial effect on magnesium corrosion [7], but an excess of Mn has been reported [8] to cause neurotoxicity and the presence of Zr is closely associated with various types of cancer [9].

Biodegradable cardiovascular stents produced from the WE alloy were successfully tested in animals [10] and the first clinical human trials have been

*Corresponding author: tel.: +420 221 911 355; fax: +420 221 911 618; e-mail address: bohumil.smola@mff.cuni.cz

Table 1. Composition of investigated alloys

Alloy	Y (wt.%)	Nd (wt.%)	Sc (wt.%)	Zn (wt.%)	Mn (wt.%)
WES	3.71	2.12	1.28	–	1.18
WEZ	3.22	2.12	–	1.22	1.45

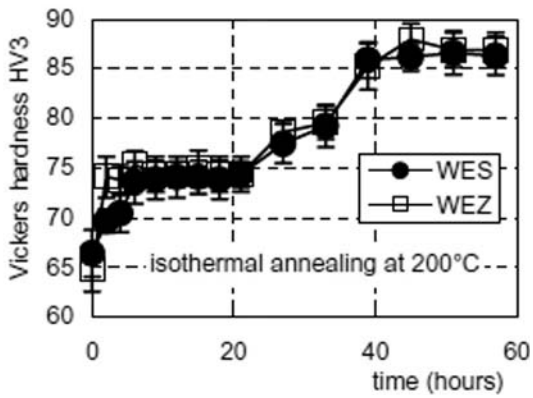

Fig. 1. Hardness HV3 response to isothermal annealing of as cast WES and WEZ alloys at 200 ℃.

performed [11]. Magnesium alloyed with rare earth elements or with their combinations is also investigated for orthopedic applications as load-bearing biodegradable implants in various designs as screws, plates, etc.

The aim of the present communication is to investigate microstructure and cell behaviour of two modifications of WE-based alloys, namely squeeze cast Mg--Y-Nd-Sc-Mn and Mg-Y-Nd-Zn-Mn alloys. Microstructure was changed by the T5 heat treatment and the as cast as well as the T5 conditions were characterized by yield tensile stress and strength at room temperature.

2. Experimental details

Alloys investigated were squeeze cast starting from pure materials and a master alloy Mg-Mn under a protective gas atmosphere (Ar + 1 % SF_6). The composition of alloys is listed in Table 1. The T5 heat treatment was determined on the base of hardness response to isothermal annealing at various temperatures for both cast alloys investigated. The treatment was finished by specimen quenching into water. Peak hardness was obtained after annealing at 200 ℃ for both alloys and the HV3 hardness developments are shown in Fig. 1. They are very similar despite the different alloying elements Sc and Zn and exhibit successively two hardening stages. Peak hardness is comparable with hardness values for the commercially used WE43 alloy in the T6 condition.

Transmission electron microscopy (TEM) and electron diffraction (ED) were carried out in JEOL JEM 2000FX microscope to determine microstructure of the alloys after the specified treatments. An analysis of phases precipitated out was also supported by energy dispersive X-ray microanalysis (EDS). The optical and the scanning electron microscopy were used in structure studies.

Tensile tests were performed at alloys in the as cast and T5 conditions at an initial strain rate of $\approx 10^{-4}\,s^{-1}$ and room temperature. Results of three tests were used to determine mean values.

Disc-shape specimens (8 mm in diameter, 3 mm thick, $\sim$ 280 mg), machined from all four studied materials were sterilized by UV radiation. Extracts of alloys were prepared according to the ISO 10993-5. Each disc was immersed in the agitated EMEM solution (60 rpm, 1.75 ml, pH = 7.2, 37 ℃) without bovine fetal serum for 5 days. Behaviour of the human osteosarcoma cell line MG63 cells (supplied by Sigma, collection ECACC) was studied in the gained extracts with the bovine fetal serum addition at 37 ℃ by means of time lapse cinematography. Cell spreading was evaluated after 1 h of the experiment, time was set to the beginning of viability experiment again and cell viability was monitored up to 24 h.

3. Results and their discussion

3.1. Development of microstructure and its influence on mechanical properties

The WES alloy has a typical cast structure with grain boundary eutectic and the mean grain size of $\sim$ 80 μm (Fig. 2). The grain boundary eutectics consists of the α-Mg matrix and β phase of fcc structure (Fig. 3) isomorphic to the Mg_5Gd equilibrium phase as was also observed in Mg-Y-Nd alloys [12]. The transient c-based centered orthorhombic phase (a = 0.641 nm, b = 2.223 nm, c = 0.521 nm) precipitates during the T5 anneal to form a dense arrangement of prismatic plates (diameter $\approx$ 40 nm, thickness $\approx$ 5 nm) in a layer of $\approx$ 3 μm along grain boundary eutectics (Fig. 4). Plates of this β' phase precipitate in grain interiors on dislocations only (Fig. 5). The observed orientation relationship to the matrix, namely $[0001]_{Mg}\,||\,[001]_{cbco}$, $\{2\bar{1}\bar{1}0\}_{Mg}\,||\,(100)_{cbco}$ is the same as observed in Mg-Gd or WE43 alloys [13].

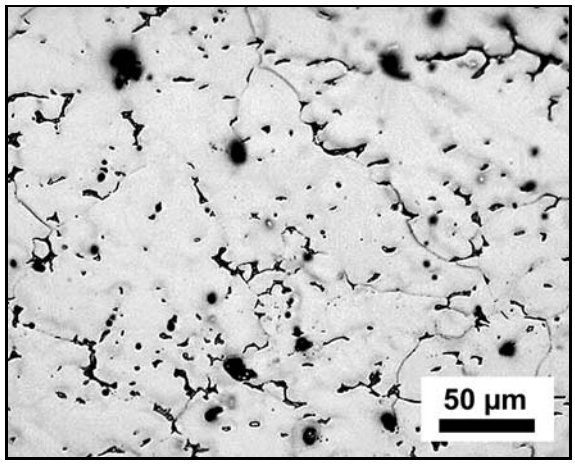

Fig. 2. Structure of as cast WES alloy.

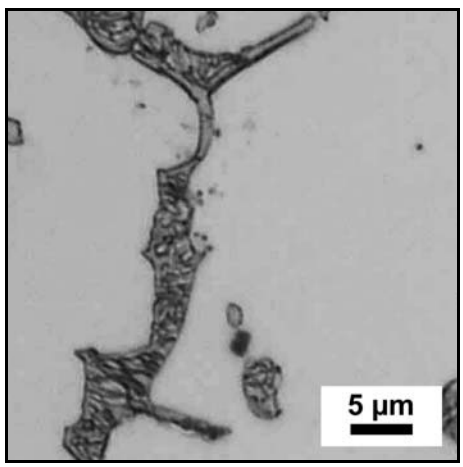

Fig. 3. Grain boundary eutectic in squeeze cast WES alloy.

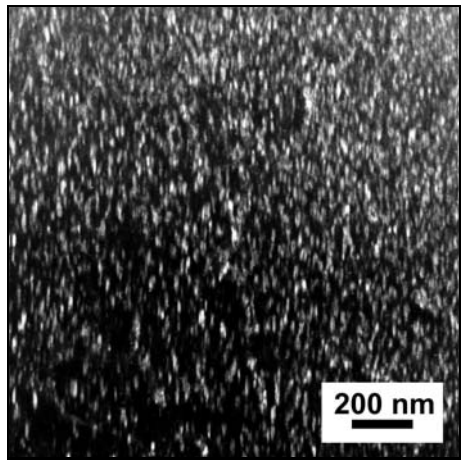

Fig. 4. Prismatic plates of C-base centered orthorhombic transient phase in WES alloy after T5 temper. $[44\bar{8}3]_{\mathrm{Mg}}$ pole, dark field in $(0\bar{4}\bar{2})_{\mathrm{cbco}}$ and $(11\bar{2})_{\mathrm{cbco}}$ reflections.

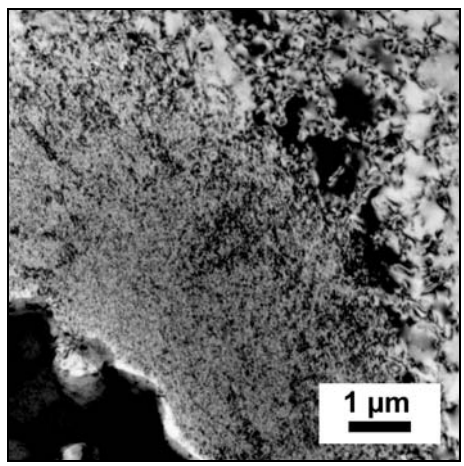

Fig. 5. Microstructure of WES alloy after T5 temper. Dense prismatic plates arrangement in the vicinity of the grain boundary eutectic.

This phase if precipitated in a form of plates is known to be the most effective precipitation hardener also in other Mg-rare earth based alloys (e.g. [14, 15]). The hardness response at the beginning of annealing at 200 ℃ in Fig. 1 implies precipitation of another former transient phase. It is most probably the DO_{19} phase analogically to other Mg-Y-Nd-type alloys [13], which precedes the cbco phase in the precipitation sequence. Basal discs of the Mn_2Sc stable phase do not precipitate during the T5 treatment, but their precipitation was proven after annealing at 250 ℃/40 h [16].

Dendritic structure as shown in Fig. 6 was observed in the as cast WEZ alloy, the mean grain size equals to ~ 80 µm and does not differ from the grain size of the WES alloy. No grain size change was observed after T5 heat treatment, again. Microstructure consists of the α-Mg matrix and the β phase. This phase with fcc structure ($a \sim 0.72$ nm) isomorphic to the equilibrium phase in Mg_3Gd alloys (known to precipitate as β_1 phase in the WE43 alloy [13]) contains significant Zn amount (~ 7 at.%). TEM revealed high density of stacking faults separated by split dislocations in the matrix (Fig. 7). They manifest themselves as intensity streaks at Mg reflections in ED patterns (Fig. 8). Figure 9 shows thin coherent hexagonal plates parallel to basal planes of the matrix with very high aspect ratio and number density formed during the T5 temper. They contain Y and Zn and were observed also in MgYZnMn alloys [17]. Prismatic plates similar to the WES alloy precipitate at 200 ℃, too. Figure 9 shows them as perpendicular to the basal plates and they are most probably responsible for the peak hardening attained.

Yield stress (YTS) and ultimate stress (UTS) determined in tensile tests at room temperature are sim-

Table 2. Yield tensile stress, ultimate tensile stress and ductility of investigated alloys in as cast and T5 condition

Alloy	YTS (MPa)	UTS (MPa)	A (%)
WES as cast	160 ± 2	206 ± 3	8.8 ± 2.6
WES T5	171 ± 1	215 ± 14	9.3 ± 0.7
WEZ as cast	150 ± 10	209 ± 5	5.4 ± 0.9
WEZ T5	156 ± 8	200 ± 10	4.3 ± 0.9

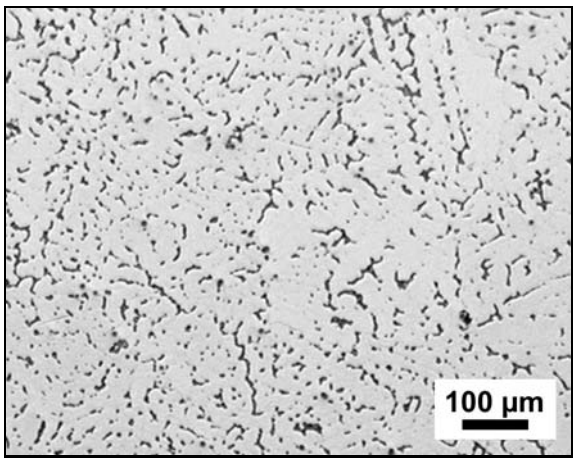

Fig. 6. Dendritic structure of as cast WEZ alloy.

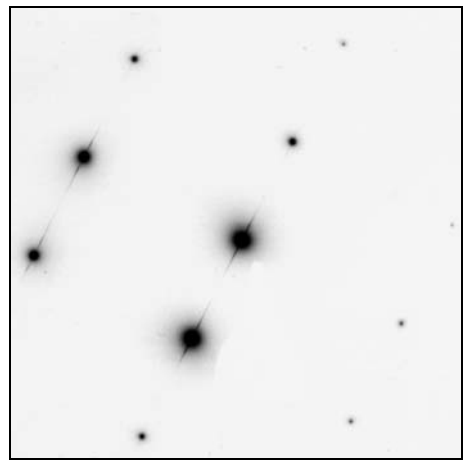

Fig. 8. $\left[10\bar{1}0\right]$ zone diffraction pattern of α-Mg matrix in as cast WEZ alloy with intensity streaks induced by stacking faults.

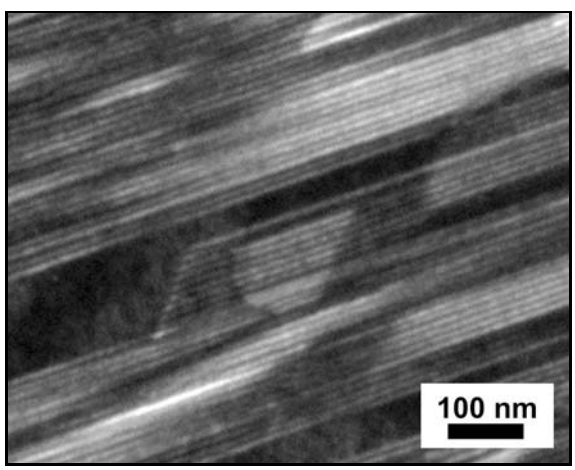

Fig. 7. Stacking faults and split dislocations in as cast WEZ alloy. Dark field weak beam image in $\left(10\bar{1}\bar{1}\right)_{\mathrm{Mg}}$ reflection near $\left[1\bar{5}4\bar{3}\right]_{\mathrm{Mg}}$ pole.

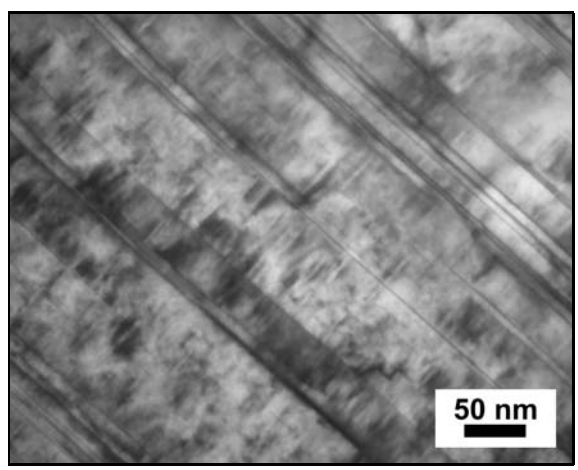

Fig. 9. Thin coherent plates parallel to matrix basal planes and prismatic C-base centered orthorhombic plates in T5 treated WEZ alloy. Bright field image, $\left[11\bar{2}0\right]_{\mathrm{Mg}}$ pole.

ilar for both alloys, too. Their values are listed in Table 2 together with ductility. The YTS and UTS values are slightly lower than those for the commercial WE43 alloy (172 MPa and 220 MPa for T6 condition) [18] but ductility improved considerably in the WES alloy compared to 2 % for the WE43 alloy in the T6 condition. Its values are lower for the WEZ alloy, but still at least two times higher than in the WE43 T6 alloy and they change considerably due to the T5 treatment neither in the WES nor in the WEZ alloy.

3.2. MG63 cells viability in extracts

Table 3 shows the relative number of MG63 cells

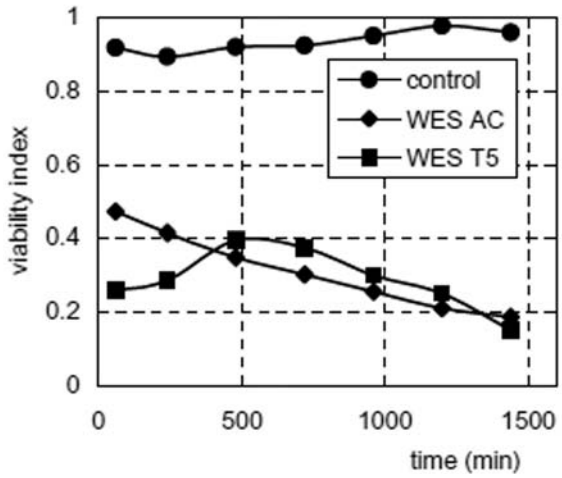

Fig. 10. Time dependence of MG63 cell viability index in WES alloy extracts.

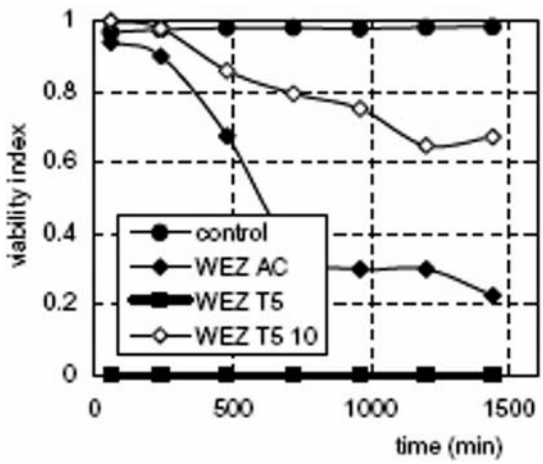

Fig. 11. Time dependence of MG63 cell viability index in WEZ alloy extracts. Notation WEZ T5 10 means 10 times diluted extract.

spread in 1 h after seeding into extracts. The cells were added to the EMEM solution without alloy extracting in the control experiment. Similar values of the spreading index, somewhat lower than in the control experiment, were found regardless the alloy composition and heat treatment.

Viability index was determined as the ratio of vital cells to the total number of cells seen in the microscope. Figure 10 shows the time dependence of viability indices for the WES alloy. Despite of the T5 treatment viability indices start at relative low values and reach very similar values after ~ 500 min of experiment further diminishing gradually to 0.2. Extracts of the as cast as well as the T5 treated WES alloy are cytotoxic for MG63 cells. Viability index of the WEZ as cast alloy shown in Fig. 11 starts at a higher value exceeding 0.6 but it decreases in the first 500 min to the WES alloys level. Even though similar values of spreading index were found for extracts of the as cast and T5 treated WEZ alloys, the extract of the WEZ alloy in the T5 condition is completely cytotoxic already after a short period of experiment – see zero values of viability index in Fig. 11.

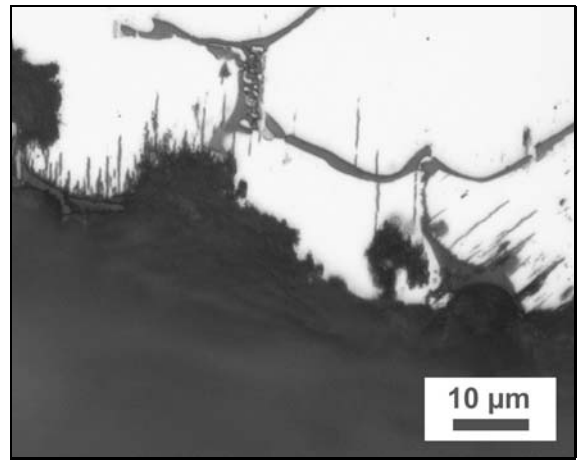

Fig. 12. WEZ alloy in T5 condition after immersion in EMEM for 5 days. Notice grain boundary eutectics and corroded regions differently oriented in different grains.

An enhanced corrosion of the WEZ T5 treated alloy in the EMEM medium was found in mutually parallel bands, their direction depends on grain orientation (Fig. 12). They are most probably connected with the thin hexagonal plates containing Zn and Y precipitated during the T5 annealing as these regions are much less pronounced in the as cast WEZ alloy and were not found in the WES alloy.

If the WEZ T5 alloy extract was diluted ten times viability of MG63 cells improves considerably. Viability diminishes with increasing experiment time, too, but it still reaches ~ 0.4 after 1400 min. It can be supposed that the used extracts are upper limits and that dynamic conditions decrease *in vivo* instantaneous concentrations of Mg and alloying elements released

Table 3. Spreading indices of MG63 cells after 1 h in alloy extracts

Alloy	Control	WES AC	WES T5	WEZ AC	WEZ T5
Spreading index	0.96	0.75	0.74	0.76	0.77

during degradation. Very promising results were obtained *in vivo* with the Mg alloyed by Mn and Zn in concentrations similar to the investigated WEZ alloy, indeed [19]. Implants were tested on rats, Mn and Zn can be absorbed by the surrounding tissue or body fluid most probably faster than Y and Nd from the WE43 alloy [5].

4. Conclusions

Two modifications of the commercial WE43 alloy, namely Mg-4Y-2Nd-1Sc-1Mn (WES) and Mg-4Y-2Nd-1Zn-1Mn (WEZ) alloys, were squeeze cast and T5 treated 40 h at 200 °C. Peak hardness comparable to that of the commercial WE43 alloy in the T6 condition was obtained. The mean grain size of ~ 80 μm as well as grain boundary decoration with eutectics in both cast alloys did not change by the T5 treatment. Grain boundary eutectics are composed of the α-Mg matrix and the β phase with fcc structure in the WES alloy and the β_1 phase with a significant Zn amount in the WEZ alloy. A high density of stacking faults characterizes the matrix in the as cast WEZ alloy.

Prismatic plates of transient c-based centered orthorhombic phase precipitate during the T5 anneal in both alloys near grain boundary eutectics. Thin coherent hexagonal plates containing Zn and Y oriented parallel to matrix basal planes replaced stacking faults in the WEZ alloy during the T5 temper.

The yield tensile stress and ultimate tensile stress values in both alloys are slightly lower than those for the commercial WE43 alloy but ductility improved considerably.

Extracts of the alloys prepared according to ISO 10993-5 are scarcely cytotolerant for MG63 cells. The total cytotoxicity was found in the extract of the WEZ T5 treated alloy. It agrees well with an enhanced corrosion of the WEZ T5 alloy in the EMEM medium. The MG63 cells viability improves considerably in the ten times diluted extract, which is more comparable with dynamic conditions *in vivo*.

Acknowledgements

The support by the Czech Science Foundation (GACR project 106/09/0407) is gratefully acknowledged.

References

[1] Witte, F., Hort, N., Vogt, C., Cohen, S., Kainer, K. U., Willumeit, R., Feyerabend, F.: Current Opinion in Solid State and Materials Science, *12*, 2008, p. 63. doi:10.1016/j.cossms.2009.04.001

[2] Castellani, C., Lindtner, R. A., Hausbrand, P., Tschegg, E., Stanzl-Tschegg, S. E., Zanoni, G., Beck, S., Weinberg, A.-M.: Acta Biomaterialia, *7*, 2011, p. 432. PMid:20804867. doi:10.1016/j.actbio.2010.08.020

[3] Staiger, M. P., Pietak, A. M., Huadmai, J., Dias, G.: Biomaterials, *27*, 2006, p. 1728. PMid:16246414. doi:10.1016/j.biomaterials.2005.10.003

[4] Zainal Abidin, N. I., Martin, D., Atrens, A.: Corr Sci, *53*, 2011, p. 862. doi:10.1016/j.corsci.2010.10.008

[5] Witte, F., Kaese, V., Haferkamp, H., Switzer, E., Meyer-Lindenberg, A., Wirth, C. J.: Biomaterials, *26*, 2005, p. 3557. PMid:15621246. doi:10.1016/j.biomaterials.2004.09.049

[6] Hanzi, A. C., Gunde, P., Schinhammer, M., Uggowitzer, P. J.: Acta Biomaterialia, *5*, 2009, p. 162. PMid:18762463. doi:10.1016/j.actbio.2008.07.034

[7] Song, G.: Corr Sci, *49*, 2007, p. 1696. doi:10.1016/j.corsci.2007.01.001

[8] Crossgrove, J., Zheng, W.: NMR Biomed, *17*, 2004, p. 544. PMid:15617053. doi:10.1002/nbm.931

[9] Purnama, A., Hermawan, H., Couet, J., Mantovani, D.: Acta Biomaterialia, *6*, 2010, p. 1800. PMid:20176149. doi:10.1016/j.actbio.2010.02.027

[10] Waksman, R., Pakala, R., Kuchulakanti, P. K., Baffour, R., Hellinga, D., Seabron, R., Tio, F. O., Wittchow, E., Hartwig, S., Harder, C., Rohde, R., Heublein, B., Andreae, A., Waldmann, K.-H., Haverich, A.: Catheter Cardiovasc Interv, *68*, 2006, p. 607. PMid:16969879. doi:10.1002/ccd.20727

[11] Zartner, P., Cesnjevar, R., Singer, H., Weyand, M.: Catheter Cardiovasc Interv, *66*, 2005, p. 590. PMid:16206223. doi:10.1002/ccd.20520

[12] Smola, B., Stulikova, I.: J. Alloys Compd., *381*, 2004, p. L1. doi:10.1016/j.jallcom.2004/02/049

[13] Smola, B., Stulíková, I.: Kovove Mater., *42*, 2004, p. 301.

[14] Nie, J. F., Muddle, B. C.: Acta Mater., *48*, 2000, p. 1691. doi:10.1016/S1359-6454(00)00013-6

[15] Apps, P. J., Karimzadeh, H., King, J. F., Lorimer, G. W.: Scripta Mater., *48*, 2003, p. 1023. doi:10.1016/S1359-6462(02)00596-1

[16] Stulikova, I., Smola, B., Pelcova, J., Vlach, M., Mordike, B. L.: Z. Metallkd., *96*, 2005, p. 823.

[17] Smola, B., Stuliková, I., Pelcová, J., Žaludová, N.: In: Magnesium Alloys and their Applications. Ed.: Kainer, K. U. Weinheim, WILEY-VCH Verlag 2007, p. 67.

[18] www.magnesium-elektron.com, 31.10.2011.

[19] Xu, L., Yu, G., Zhang, E., Pan, F., Yang, K.: J Biomed Mater Res, *83A*, 2007, p. 703. PMid:17549695. doi:10.1002/jbm.a.31273